Applied Catalysis A: General 528 (2016) 59–66

Contents lists available at ScienceDirect

Applied Catalysis A: General

journal homepage: www.elsevier.com/locate/apcata

Isosorbide production from sorbitol over porous zirconium phosphate catalyst

Dong Cao[a], Bo Yu[b], Shaoyin Zhang[a], Li Cui[a,*], Jianghua Zhang[a], Weijie Cai[a,*]

[a] Faculty of Light Industry and Chemical Engineering, Dalian Polytechnic University, 116023 Dalian, China
[b] College of Materials Science and Engineering, Dalian Jiaotong University, 116023 Dalian, China

ARTICLE INFO

Article history:
Received 26 May 2016
Received in revised form
20 September 2016
Accepted 26 September 2016

Keywords:
Isosorbide
Sorbitol
Zirconium phosphate
Dehydration

ABSTRACT

A porous zirconium phosphate catalyst prepared by hydrothermal method was studied for the dehydration of sorbitol to isosorbide under water-free conditions. Various characterization techniques such as XRD, Raman, SEM, NH_3-TPD and Pyridine adsorption etc were conducted to determine the textural and acidic properties of the catalyst so as to build the relationship between catalytic performance and catalyst structure. In screening tests with other solid acids, the as-prepared ZrP sample exhibited the promising catalytic behavior for isosorbide production probably assigned to its high surface area, porous structure and the adequate Brönsted acid sites. Full sorbitol conversion with as high as 73% isosorbide selectivity could be obtained at mild conditions (210 °C, 2 h). Noticeably, the ZrP catalyst could be repeatedly used without any obvious deactivation. Generally, the ZrP catalyst studied in this work possessed a great potentiality as an efficient heterogeneous solid acid catalyst for isosorbide production to diminish the application of homogeneous mineral acid.

1. Introduction

Recently, great efforts have been devoted to the catalytic conversion of renewable biomass and/or biomass-derived feedstocks to fine chemicals and liquid fuels to fulfill the sustainable development [1–5]. In particular, sorbitol, known as one of the top twelve platform chemicals, has achieved considerable attention and has a special application in chemicals, fuels, commodity to partially replace conventional fossil fuels [6–9]. Meanwhile, sorbitol as an important biomass-derived material could be readily produced from enormous cellulose or lignocellulose [10,11]. Among the various sorbitol-derived chemicals, isosorbide(1.4:3.6-di-anhydrohexitol), a product of sorbitol dehydration, is regarded as one of the most promising derivates considering its typical application in the polymer and medicine field because of its rigid molecular structure and chiral centers [12,13]. Notably, incorporation of isosorbide monomer into the poly(ethyleneterephthalate) polymer (PET) might greatly enhance its glass transition temperature. Currently, isosorbide also acted as an promising alternative of bisphenol A in the synthesis process of epoxy resins or polycarbonate to eliminate environmental pollution [14–16].

Up to date, many research has been conducted on the sorbitol dehydration to isosorbide in order to develop an efficient catalyst [17]. From the standpoint of environmentally-benign, Yamaguchi et al. studied the dehydration of sorbitol in high temperature liquid water without the addition of any acid catalysts and the maximum isosorbide yield was ca.57% at 317 °C for 1 h [18]. In contrast, the results were still not satisfactory for the industrial application due to high temperature and pressure. Similarly, Almeidat et al. selected a molten $ZnCl_2$ hydrate medium as both solvent and catalyst and 100% sorbitol conversion with ca.85% selectivity of isosorbide was obtained at 200 °C. It is noteworthy that this process possessed several drawbacks such as solvent recover and remarkable salt formation [19]. Otherwise, mineral acids like HCl and H_2SO_4 as homogeneous catalysts showed a satisfied performance. Fleche et al. revealed that 77% isosorbide yield could be achieved at 135 °C over liquid H_2SO_4 catalyst [20]. Moreover, major obstacles for the process using the liquid acids were difficult separation of isosorbide from reaction system, equipment corrosion and environmental pollution caused by any discharge of acids. Hence, a great interest has been arisen on the development of heterogeneous solid acid catalyst to replace conventional min-

* Corresponding authors.
E-mail addresses: cuili@dlpu.edu.cn (L. Cui), caiwj@dlpu.edu.cn (W. Cai).

http://dx.doi.org/10.1016/j.apcata.2016.09.017
0926-860X/

eral acids because of their environmentally friendly nature with respect to easy separation, less corrosiveness and waste [21–23]. Consequently, several solid acid catalysts such as sulfuated copper oxide [24], supported heteropolyacid [25], zeolites [26,27], superhydrophobic mesoporous acid (P-SO_3H) [28], Amberlyst-15 [29] and metal phosphates [30,31] have been selected in the catalytic dehydration of sorbitol. Nevertheless, the process using heterogeneous catalysts still has not been commercialized. Most of the studied solid acid samples normally need higher reaction temperature and more reaction time to achieve satisfactory isosorbide yield leading to high operation cost. Additionally, zeolite based catalysts suffered from the readily deactivation because of the structure distortion during the reaction process [32]. Some catalysts also exhibited less stability due to serious leaching of acid sites and several other ones were toxic like tin phosphate [33,34]. Therefore, it is desirable to development an efficient catalyst for the dehydration of sorbitol that could be operated at moderate conditions.

Generally, zirconium phosphate is one of the most promising solid acids for dehydration reactions. Much efforts have been conducted on zirconium phophate, considering its several merits such as nontoxicity, thermal stability, eco-friendly, strong acidity, recycling etc [35–37]. Moreover, many literatures have described the synthesis of high-valued chemicals from biomass-derived feedstocks over zirconium phosphate [38,39]. Meanwhile, the incorporation of enormous nanopores in solid acid catalysts might remarkably improve the mass transfer of reactants and facilitate the exposure of acid sites leading to better catalytic behavior in various reactions like isomerisation, dehydration, esterification etc. To the best of our knowledge, the application of zirconium phosphate with porous structure for the catalytic dehydration of sorbitol has still been in its infancy. Rusu et al. [40] investigated the isosorbide production using trivalent and quadrivalent phosphate as solid acid catalysts and the best catalytic performance was obtained over boron phosphate sample.

In this work, a zirconium phosphate catalyst with porous structure was successfully synthesized by a sol-gel process using P123 as a sacrifice template and elaborately investigated to design an effective, environmental-benign catalyst for isosorbide production. Catalytic parameters (reaction temperature, reaction time, catalyst amounts etc) were studied in detail and the results were compared to other solid acid catalyst. Additionally, a systematic characterization of the as-prepared catalyst (XRD, SEM, TEM, FTIR, pyridine adsorption, NH_3-TPD, BET etc) were conducted to establish a relationship between catalyst textural properties and catalytic behavior.

2. Experimental

2.1. Catalyst preparation

Zirconium phosphate catalyst was synthesized by a sol-gel self-assembly process [41]. Typically, aqueous H_3PO_4 was slowly added into an solution of $ZrOCl_2$ (P/Zr = 2/1, molar ratio) under magnetic stirring (800 rpm). Another ammonia solution was then dropped into the mixture until the pH value was at around 5.0. The precipitate was thoroughly filtered and washed with hot deionized (DI) water until no chloride ions were detected. Under continuous stirring, the obtained precipitate was then added into an aqueous solution of Pluronic P123 (PEG-PPG-PEG triblock copolymer) which was employed as the structural directing agent. Finally, aqueous H_3PO_4 was dropwised under stirring and the resultant gel was poured into a Teflon-lined stainless steel autoclave at 40 °C for 24 h and at 75 °C for another 24 h. After filtration and thorough washing with hot DI water, the precipitate was dried at 90 °C overnight and calcined at 450 °C for 6 h in static air. The as-prepared zirconium phosphate was denoted in a general form ZrP in the following discussion.

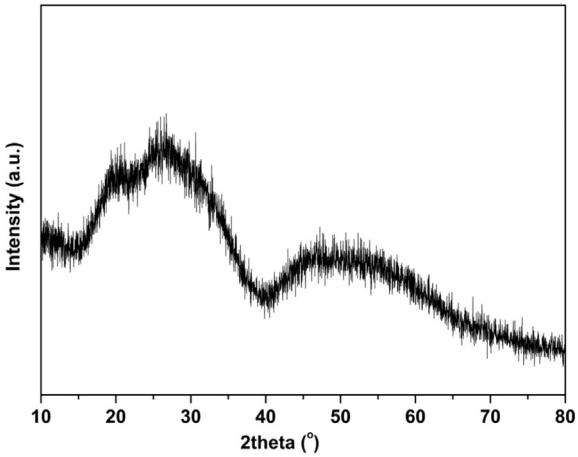

Fig. 1. XRD pattern of the ZrP catalyst.

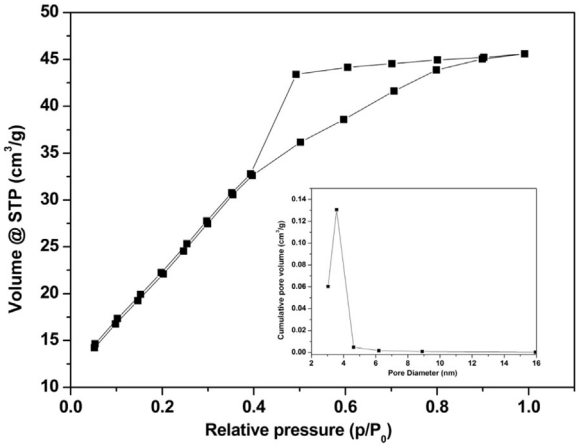

Fig. 2. Nitrogen adsorption-desorption isotherm of the ZrP catalyst.

2.2. Catalyst characterization

X-Ray diffraction patterns (XRD) were recorded in the 2θ range of 10–80° on a Rigaku X-3B diffractor with Cu K_α radiation source operating at 40 kV and 60 mA.

The surface area and porous structure was measured by Nitrogen adsorption-desorption at −196 °C on an ASAP 2010 Micrometrics apparatus. Before analysis, the catalyst was outgased at 300 °C for 3 h under N_2 flow (50 mL/min) to remove the adsorbed impurities on the catalyst surface.

Fourier transform infrared (FT-IR) spectra was conducted on a Digilab FTS 3100 FTIR spectrometer. Prior to measurement, the investigated ZrP sample was dried at 100 °C over night and then pressed into a wafer by diluting the catalyst with KBr (spectroscopic grade).

Infrared (IR) spectra of pyridine adsorption was also operated on a same Digilab FTS 3100 FTIR spectrometer to explore the acid types of ZrP catalyst. Firstly self-supported wafers of the catalysts were placed into an IR cell and then the disk was heated at 300 °C for 1 h under vacuum conditions to remove adsorbed impurities over the catalyst surface. After quenching down to room temperature, IR spectrum was recorded as background and pyridine vapor was then added until equilibrium was achieved. Subsequent evacuation was performed at 150 °C under vacuum conditions followed by spectral

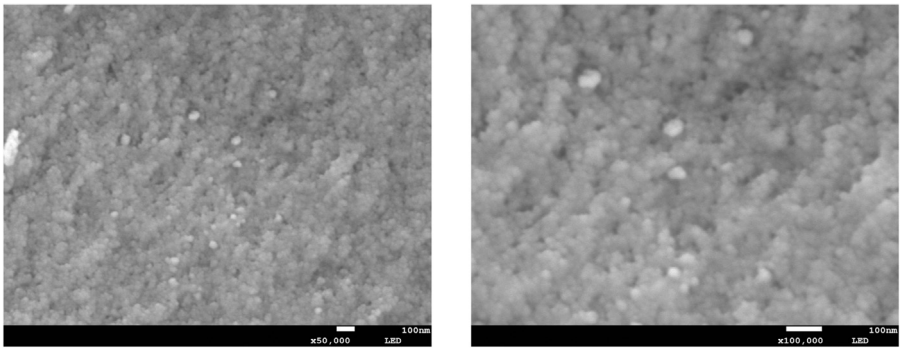

Fig. 3. SEM micrographs of the ZrP catalyst.

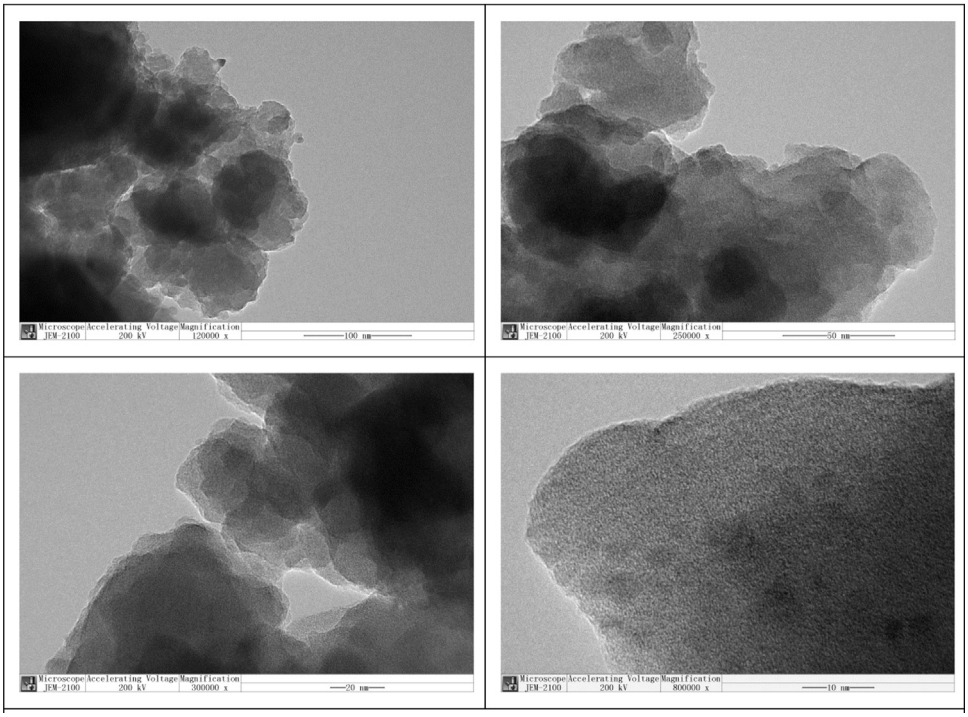

Fig. 4. TEM images of the ZrP catalyst.

acquisitions. The presented spectra was obtained by subtracting the spectra recorded before and after pyridine adsorption. The ratio of strong Brönsted acid sites to Lewis sites was semi-quantified based on the peak areas centered at 1540 cm^{-1} and 1450 cm^{-1}, respectively [42].

Temperature-programmed desorption of ammonia (NH_3-TPD) measurement was carried out to further estimate the total acidity of catalysts. Before adsorption, catalyst loaded in a quartz reactor was pretreated at 300 °C for 1 h under He flow (50 mL/min). After cooling down to room temperature, NH_3 adsorption was performed by switching He flow to a stream of 10 vol% NH_3/He (50 mL/min) and maintaining the temperature for 0.5 h. Then, the weakly adsorbed NH_3 was removed under He flow (50 mL/min) for another 0.5 h. NH_3-TPD was conducted under He flow (50 mL/min) by increasing the temperature to 800 °C at a heating rate of 5 °C/min and the desorbed NH_3 molecules were continuously monitored using an on-line mass spectrometry (Inficon quadrupole).

The amounts of desorbed NH_3 at different temperatures were calculated based on the relative areas of the deconvolution peaks, as follows:

$$D = D_{Total} * (A/A_{Total}) * 100\% \quad (1)$$

where D_{Total} (mmol/g) is the total quantity of desorbed NH_3; A is the area of a deconvolution peak and A_{Total} is the total areas of all the deconvolution peaks.

The morphology of ZrP catalyst was investigated by Field-emission scanning electron microscope (FESEM) using JEOL JSM-6460LV. Before analysis, the powdered catalyst was supported on stubs and coated by Au using plasma.

Transmission electron microscope (TEM) images were obtained using JEM-2100 microscope operating at 200 kV. Prior to measurement, the sample was ultrasonically suspended in ethanol. Then a drop of the mixture was deposited onto a thin carbon film supported on a standard copper grid and dried in air.

The actual composition of ZrP catalyst was measured using an inductively coupled plasma atomic emission spectrometer (ICP, PLASMA-SPEC-II).

2.3. Catalytic measurements

The catalytic activities of ZrP sample in dehydration of sorbitol were tested in a stainless-steel batch reactor (60 mL) without the addition of any solvent. Particularly, a mixture of pure sorbitol

and catalyst was added into the autoclave and purged with N_2 for several times to remove air. Then, the reactor was heated under magnetically stirring at 800 rpm. After the reaction, the reactor was quickly quenched in an ice-water bath and a small amount of DI water was added. Subsequently, the mixture was filtrated and the obtained liquid product was analyzed by HPLC (Wates e2695) with an Shodex SUGAR SC1011 column (8 × 300 mm). The operating temperature of column and detector was selected to be 70 °C and 35 °C, respectively. Distilled water was selected as mobile phase (0.6 mL/min). The same experimental procedures were repeated at least two times to verify the reproducibility. The deviation of the results was observed below 5% ruling out the effect of the experimental error.

Sorbitol conversion and isosorbide selectivity was calculated according to the following equation:

$$C_{sorbitol}\% = (\text{moles of reacted sorbitol/mol of initial sorbitol}) * 100\% \quad (2)$$

$$S_{isosorbide}\% = (\text{moles of carbon in the produced isosorbide/mol of carbon in the reacted sorbitol}) * 100\% \quad (3)$$

2.4. Catalyst recyclability

The reusability of the ZrP catalyst was determined in order to assess its stability for the possible industrial application. The tests were conducted under the identical experimental conditions as mentioned above. After each reaction, the used catalyst was filtered and thoroughly washed with hot DI water and dried at 90 °C over night. The recovered catalyst was finally calcined at 450 °C for 2 h in static air for the next run.

3. Results and discussion

ICP result indicated that the resulting molar ratio of P to Zr in the as-prepared ZrP catalyst was ca.1.93, which was very close to the stoichiometry indicating no loss of the active component occurred during the synthesis process of the catalyst. Fig. 1 presents the XRD patterns of the ZrP sample. Only two broad peaks in the 2θ ranges of 10–40° and 40–70° respectively were observed suggesting its amorphous structure in good agreement with the previous literature [43]. No characteristic diffraction peaks assigned to zirconium phosphate and/or zirconia were observed.

The textual properties of the ZrP catalysts were further studied using nitrogen adsorption-desorption isotherms as presented in Fig. 2. The specific surface area and average pore diameter was around 148 m^2/g and 3.57 nm, respectively. Interestingly, three different stages were observed from the isotherm curve. The first stage was observed at $p/p_0 < 0.4$, the second one was observed in the region of $0.4 < p/p_0 < 0.9$ and the third one was observed at $p/p_0 > 0.9$. Notably, the N_2 adsorption-desorption isotherms corresponded to a type IV isotherm with a typically hysteresis loop implying the porous structure of the synthesized ZrP catalyst. It was generally accepted that the observed hysteresis loop from $p/p_0 = 0.4$ was assigned to the capillary condensation occurring in the mesopores [44–46]. Additionally, the distribution of pore size calculated by the Cranston and Inkley method (inserted in Fig. 2) also elucidated a narrow pore size range centered around 3.5 nm supporting the mesoporous nature of the ZrP sample.

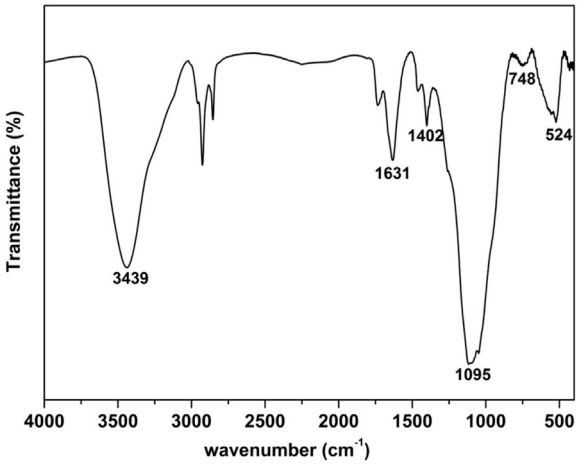

Fig. 5. FT-IR spectra of the ZrP catalyst.

The microscopy of the ZrP catalyst was firstly analyzed using SEM and the results were shown in Fig. 3. Apparently, both the spherical particles with sizes in the range of 10–20 nm and the worm like porous structure were observed which were highly in line with the previous XRD result. The TEM micrograph, depicted in Fig. 4 also revealed that the ZrP sample consisted of conglomerated particles which connected each other and a clear pore channel was observed confirming the formation of porous structure. It was noted that an average pore size of ca.3–5 nm was in line with the value achieved from BET results. And it also demonstrated a short range order of porous structure. Combining with the BET analysis, the wormlike structure might have good interconnection to result into the high surface area and pore volume observed.

Fig. 5 shows the FT-IR spectra of the ZrP catalyst. An intense band in the range of 1000–1100 cm^{-1} was attributed to the P-O symmetrical vibration of $-PO_4$ group [47] and the spectral band at ca.524 cm^{-1} was assigned to the Zr—O stretching vibration [48]. A slight peak at ca.748 cm^{-1} corresponded to the P—O—P vibration suggesting the formation of P—O—P band. Moreover, the bands centered at ca.3439 and 1631 cm^{-1} were associated to the —OH vibration and the peak located at ca.1402 cm^{-1} was due to bending vibration mode of —OH groups in good consistent with the previous reports [49]. These —OH groups might be the origin of the Brönsted acidy of ZrP catalyst. The clear peak at ca.3439 cm^{-1} also could not rule out the partial contribution of the stretching vibration of adsorbed lattice water molecules.

Briefly, the surface acidity is one of the important factors for solid acid catalysts to catalyze dehydration reaction. It is recognized that FT-IR spectra of pyridine adsorption is an effective technique to determine the types of acid sites on the catalyst surface. Typically, pyridine molecules formed pyridinium ions with Brönsted acid centers. In contrast, they were coordinated with Lewis acid sites because of their electron-pair deficient property [50]. The pyridine adsorption spectra of the ZrP catalyst is shown in Fig. 6 revealing the co-existence of Brönsted and Lewis acid sites. An intense band at around 1540 cm^{-1}, typical of pyridinium ions, confirmed the presence of Brönsted acid sites. Another strong peak at ca.1446 cm^{-1} was attributed to the pyridine adsorption on Lewis sites and the peak at ca.1489 cm^{-1} revealed the presence of a mixture of Brönsted and Lewis acid sites [51]. It was noted that the intensity of the adsorption peaks corresponded to the quantity of acid sites. Additionally, the ratio of Brönsted and Lewis sites was calculated according to the method described by Emeis [52]. The result indicated that most of the acid sites (ca.62%) were Brönsted acid sites. Meanwhile, upon further heating to 400 °C, only a slight decline of the intensity of the peak at ca.1540 cm^{-1} was observed

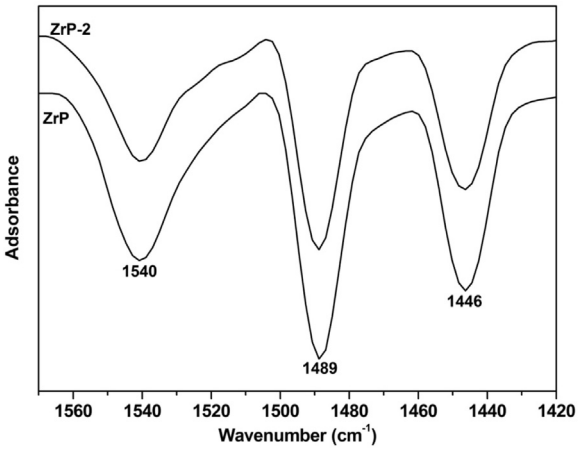

Fig. 6. Pyridine-adsorption FTIR of the ZrP catalysts.

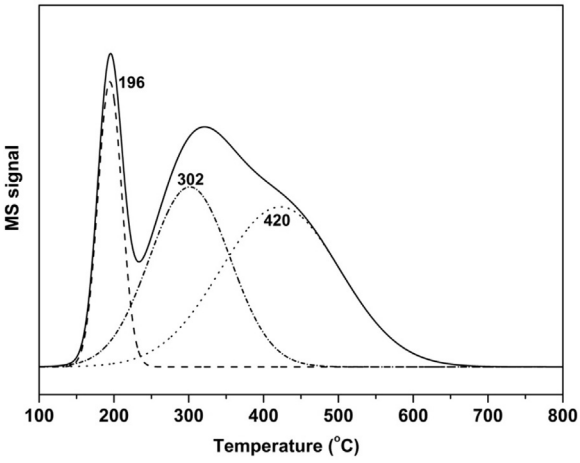

Fig. 7. NH_3-TPD profiles of the ZrP catalyst.

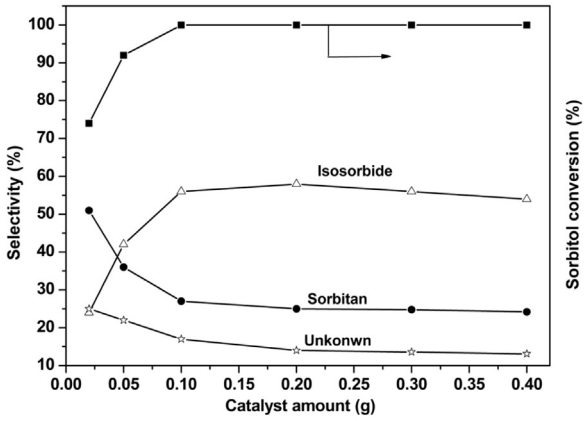

Fig. 8. Effect of catalyst amount on sorbitol dehydration. (Reaction temperature:190 °C, reaction time:1 h, sorbitol:1 g).

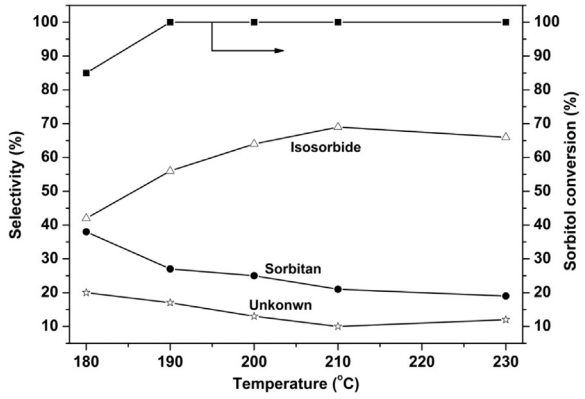

Fig. 9. Effect of the reaction temperature on sorbitol dehydration. (Reaction time:1 h, sorbitol:1 g, catalyst:0.1 g).

indicating the stability of Brönsted acid sites in the ZrP catalyst. In contrast, a remarkable decrease for the adsorption peaks located at ca.1446 cm^{-1} revealed the diminishment of Lewis acid sites. Dabbawala et al. reported that the sorbitol dehydration to isosorbide was greatly affected by catalyst acidity and types of acid sites [53]. Therefore, a great number of Brönsted acid sites on the surface of the ZrP catalyst could efficiently enable the dehydration of sorbitol occur.

NH_3-TPD was also conducted to quantify the total acidity of the investigated ZrP catalyst. Normally, the temperature of NH_3-desorption was associated with the acidity strength; the higher desorption temperature corresponded to the stronger acid sites. The amounts of the acid sites could be obtained from the quantities of desorbed NH_3 which was calculated based on the peak areas of the TPD profile [54]. As shown in Fig. 7, NH_3 desorption started from ca.150 °C and rapidly increased to a maximum value at around 196 °C. Additionally, a broad band at ca.330 °C with a clear hump at 455 °C was observed and the NH_3 desorption was not diminished until 700 °C. Generally, the acid sites on the catalyst surface was denoted as weak, medium and strong ones in the desorption region of 150–250 °C, 250–400 °C and >400 °C, respectively [55]. The bands appeared in the TPD profile could be further deconvoluted into several distinct peaks with various maximum from 100 to 700 °C. Apparently, the peak at 196 °C supported the presence of weak acid sites and the other two peaks at ca.302 and 420 °C was assigned to the existence of medium and strong acid sites, respectively. The calculated acidity resulted in the following order: Weak (0.415 mmol/g) <Medium (0.887 mmol/g) <Strong (1.167 mmol/g). The concentration of the medium and strong acid sites was around 48% and the total acidity of the ZrP catalyst was around 2.47 mmol/g, which was comparable with the values described in the previous literature [45].

The ZrP catalyst might be potential solid acid catalysts toward many acid-catalyzed reactions considering their reasonable acid properties. Therefore, the as-prepared ZrP was selected as a promising catalyst for the selective dehydration of sorbitol to isosorbide under water free conditions in this work. The optimized reaction conditions such as the catalyst amount, reaction temperature and reaction time, were explored. Initially, a blank test was conducted and compared with the results using ZrP as catalyst to elucidate the key role of catalyst. At 190 °C, sorbitol conversion of the blank reaction was only ca.19%. along with trace amounts of targeted isosorbide (<5%). In contrast, the presence of heterogeneous solid acid ZrP catalyst greatly improved sorbitol conversion (from 19% to 100%) and isosorbide selectivity (ca.56%) under the identical reaction conditions. The results clearly revealed that ZrP catalyst remarkably facilitated sorbitol conversion to isosorbide. Generally, it indicated that both the porous structure of the as-prepared ZrP catalyst and the strong acidity improved the mass transfer and provided abundant accessible active sites for the reactants leading to the satisfactory catalytic behavior in the dehydration of sorbitol.

Catalyst dosage is one of the key characteristics for the kinetics of conversion and is necessary to be optimized in order to achieve a satisfied catalytic behavior. Hence, the influence of catalyst amount was studied by changing the catalyst loading while keeping other experimental conditions constant and the results were shown in

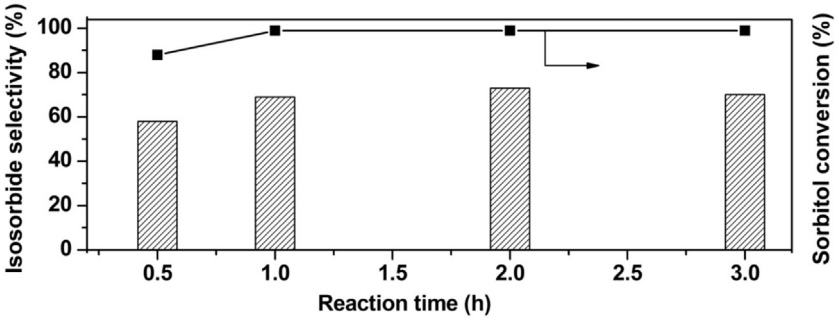

Fig. 10. Effect of the reaction time on sorbitol dehydration. (Reaction temperature:210 °C, sorbitol:1 g, catalyst:0.1 g).

Fig. 8. According to the data, the main observed products were isosorbide and 1,4-sorbitan while trace amount of 1,5-sorbitan by-product was also detected. Other non-indentified compounds were denoted here as 'unknown'. It was noted that complete conversion of sorbitol was achieved when the catalyst dosage was 0.1 g. In addition, the isosorbide selectivity progressively increased upon raising catalyst amount up to 0.2 g and a slightly decline was observed with further increasing the catalyst dosage. The main reason might be due to the excessive amounts of acid sites which were much preferred for the consequent formation of polymer and/or humin by-product. Yamaguchi et al. described that the self-polymerization of isosorbide or cross-polymerization with other by-products corresponded to the decline of isosorbide selectivity [18]. Moreover, the decrease of sorbitan selectivity indicated that the conversion of sorbitol to isosorbide mainly consisted of two consecutive dehydration reactions with sorbitan as an intermediate which agreed well with the previous literature [56]. Considering the operating cost, the optimum amount of the catalyst was selected to be 0.1 g for the later studies.

In the next step, Fig. 9 shows the effect of reaction temperature for the catalytic dehydration of sorbitol which were investigated in the temperature range from 180 °C to 230 °C. 100% sorbitol conversion was observed at 190 °C. With respect to the product composition, isosorbide selectivity rapidly increased to a maximum value (ca. 69%) from 180 °C to 210 °C. In addition, the selectivity of sorbitan was steadily declined from 37% to 21% supporting sorbitan was an intermediate as discussed in the previous studies [53]. Upon further heating to 230 °C, the formation of humin by-products led to the slight decrease of isosorbide selectivity.

The tests were also carried out in the region from 0.5 to 3 h to elucidate the influence of reaction time. The results (Fig. 10) clearly indicated that the reaction time possessed a considerable impact on the sorbitol conversion and the selectivity to the targeted isosorbide. Only 89% sorbitol conversion with 58% selectivity of isosorbide were observed at the initial 0.5 h. When reaction time was further prolonged to 2 h, an obvious increase of isosorbide selectivity (73%) with full sorbitol conversion was observed. Beyond of 2 h reaction time, a slightly decline of the isosorbide selectivity from 73% to 70% occurred. The reaction results revealed that a part of isosorbide might be unstable on the prolonged time taking place self-polymerization reaction to form humins by-product. Therefore, the optimum experimental conditions of current work might be operated at 210 °C and 2 h with a mass ratio of catalyst to sorbitol 1:10. Both increasing the reaction temperature and/or extending the reaction time hardly exhibited any promoted influence on the catalytic performance.

In order to elucidate the role of solid acid catalyst in the dehydration of sorbitol, several commercially solid acid catalysts such as Amberlyst-15, Nifon and Niobic acid were also investigated by using the same amount of catalyst under identical conditions for comparison purpose. Moreover, another ZrP sample was synthesized by the conventional precipitation procedure without the addition of P123 template. Here, the obtained reference catalyst was denoted as ZrP-2 and also tested for reaction activity. From the presented results (Fig. 11), it was clearly observed that the as-prepared porous ZrP catalyst exhibited the exceptional catalytic performance, producing isosorbide in 73% yield with 100% conversion of sorbitol, which was in contrast to the lower activity of ZrP-2 sample (59% yield of isosorbide). Although Amberlyst-15 sample showed the comparative sorbitol conversion, its isosorbide selectivity was much less than the value of ZrP sample. In addition, the concentration of sorbitan intermediates was much higher in the case of Nafin and Niobic acid catalysts and an incomplete sorbital conversion was observed. As described in the previous literature [21,53], the isosorbide production from sorbitol was greatly affected by the strength of catalyst acidity and types of acid sites. Normally, the samples containing strong Brönsted acid sites were more efficient for isosorbide production. Therefore, more Brönsted acids sites in ZrP catalyst compared to the other investigated catalysts might be one of the reasons for its better catalytic behavior. As presented in Fig. 6, both of the ZrP and ZrP-2 samples exhibited the similar pyridine adsorption peaks. However, the peaks corresponded to the Brönsted acids sites for the ZrP catalyst were obviously higher than the values of the ZrP-2 sample. That means the higher amount of Brönsted acids sites in porous ZrP catalyst. The appearance of more sorbitan intermediate for the other ones further supported this guess. Additionally, the special behavior of ZrP catalyst might be also attributed to its high surface area and porous structure, which enabled the sorbitol molecules easily approach on acid sites due to the lack of diffusion limitation [57]. Thus, the screening tests with various solid acid catalysts clearly indicated that the porous ZrP catalyst in this work possessed pretty potential in dehydration sorbitol to isosorbide.

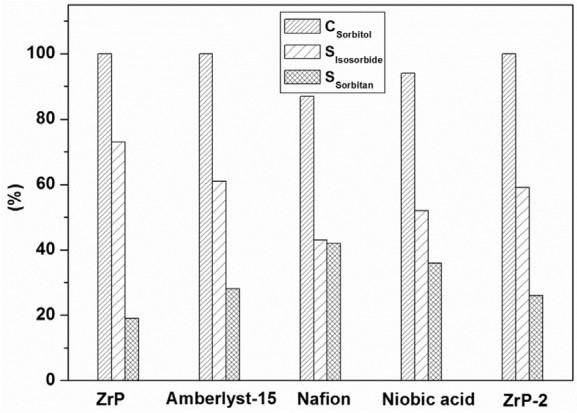

Fig. 11. Comparison of catalytic performance of ZrP sample with other solid acid catalysts. (Reaction temperature:210 °C, reaction time:2 h, sorbitol:1 g, catalyst:0.1 g).

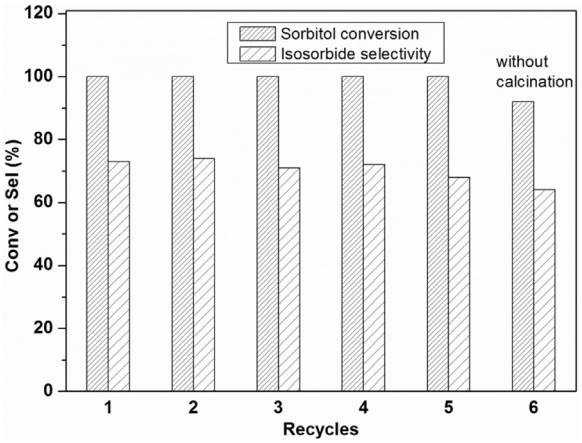

Fig. 12. Recyclability test of the ZrP catalyst for sorbitol dehydration reaction. (Reaction temperature:210 °C, reaction time:2 h, sorbitol:1 g, catalyst:0.1 g).

Catalyst recyclability is of great importance from the standpoint of the industrial operation. Therefore, the reusability of the ZrP catalyst has been tested at 210 °C for 2 h with 0.1 g of catalyst and the results are showed in Fig. 12. Sorbitol conversion was observed still 100% up to the fifth run. With respect to isosorbide selectivity, only a slight decline (from 73% to 68%) occurred up to fifth test indicating the reusability of the catalyst. Additionally, ICP analysis revealed that no obvious leaching of Zr and/or P occurred after the repeated cycles. Another main reason for the catalyst deactivation was that impurities (like polymer or humins) deposited on the catalyst surface might occupy a part of surface acid sites leading to the decline of catalytic reactivity. Based on this hypothesis, ZrP catalyst after the first run was directly used for the next test without the calcination treatment. As shown in Fig. 12, catalyst afforded a decrease selectivity (64%) of isosorbide and an incomplete sorbitol conversion (92%). Simultaneously, no obvious Zr or P was detected by ICP analysis in the solution with catalyst separated after reaction. In contrast, the coke deposition was clear from TG analysis (not shown) and as high as 13% weight loss except water occurred. The results revealed that the deposition of the carbonaceous impurities on the catalyst surface might be the main cause of the deactivation. The observed slight decrease (from 73% to 68%) was probably due to the residual humin by-product that could not be burned at 450 °C. TG result revealed that ca.1.6% weight loss from 450 °C to 800 °C was observed. However, the calcination process regenerated the most activity of catalyst. Therefore, ZrP sample could be repeatedly used as solid acid without obvious loss of the activity.

In summary, all of the above results revealed that the ZrP catalyst presented great potentiality in sobitol conversion to isosorbide with high conversion, selectivity and stability, which was important for the wide application of ZrP catalyst in biomass conversion. This promising catalytic performance was mainly attributed to its high acidity because of the incorporation of zirconium and phosphorus on the pore surface and the high external surface area which exposed a great quantity of active acid sites at the surface of the catalyst as described by the previous literature [46].

4. Conclusions

This work mainly investigated the catalytic dehydration of sorbitol to isosorbide over a porous ZrP catalyst under water free conditions. It was proposed that the isosorbide yield greatly affected by natures of acid sites and porous structure of the catalyst. A great number of Brönsted acid sites on the catalyst surface was more favorable for isosorbide formation compared to Lewis ones. Meanwhile, the porous structure of the catalyst promoted the accessibility of reactant molecules to acid sites. Therefore, a maximum yield of isosorbide as high as 73% could be achieved under an optimum condition of 210 °C and 2 h. Otherwise, ZrP was an recyclable catalyst without clear deactivation during five consecutive tests. The positive result in this work may shed light on the development of efficient catalysts for biomass conversion achieving the goal of synthesis of high-valued chemicals from renewable biomass and/or biomass-derived feedstocks.

Acknowledgements

We gratefully acknowledge the financial support from Program for National Natural Science Foundation of China (Grant no. 21303185), Liaoning Excellent Talents in University (Grant no. LJQ2014053) and Open Project Program of the State Key Laboratory of Fine Chemicals, Dalian University of Technology (Grant no. KF1416).

References

[1] C.Z. Li, X.C. Zhao, A.Q. Wang, G.W. Huber, T. Zhang, Chem. Rev. 115 (2015) 11559–11624.
[2] X. Lei, F.F. Wang, C.L. Liu, R.Z. Yang, W.S. Dong, Appl. Catal. A 482 (2014) 78–83.
[3] B.O. Beeck, M. Dusselier, J. Geboers, J. Holsbeek, E. Morre, S. Oswld, L. Giebeler, Energy Environ. Sci. 8 (2015) 230–240.
[4] Y. Liu, L. Chen, T. Wang, Q. Zhang, C. Wang, J. Yan, L. Ma, ACS Sustain. Chem. Eng. 3 (2015) 1745–1755.
[5] M.C. Alarcón, A. Corma, S. Iborra, J.P. Gómez, Appl. Catal. A 346 (2008) 52–57.
[6] J. Zhang, J.B. Li, S.B. Wu, Y. Liu, Ind. Eng. Chem. Res. 52 (2013) 11799–11815.
[7] J. Xi, Q. Xia, Y. Shao, D. Ding, P. Yang, X. Liu, G. Lu, Y. Wang, Appl. Catal. B 181 (2016) 699–706.
[8] F. Aiouache, L. McAleer, Q. Gan, A.H.A. Muhtaseb, M.N. Ahmad, Appl. Catal. A 466 (2013) 240–255.
[9] I.M. Leo, M.L. Granados, J.L.G. Fierro, R. Mariscal, Appl. Catal. B 185 (2016) 141–149.
[10] A. Corma, S. Ibora, A. Velty, Chem. Rev. 107 (2007) 2411–2502.
[11] J. Xu, Y. Zhang, Q. Xia, X. Liu, J. Ren, G. Lu, Y. Wang, Appl. Catal. A 459 (2013) 52–58.
[12] Y. Yang, Z. Xiong, L. Zhang, Z. Tang, R. Zhang, J. Zhu, Mater. Des. 91 (2016) 262–268.
[13] H. Kobayashi, H. Yokoyama, B. Feng, A. Fukuoka, Green Chem. 17 (2015) 2732–2735.
[14] C. Lorenzini, D.L. Versace, E. Renard, V. Langlois, React. Funct. Polym. 93 (2015) 95–100.
[15] Y.S. Eo, H.W. Rhee, S. Shin, J. Ind. Eng. Chem. 37 (2016) 42–46.
[16] J.M. Sadler, F.R. Toulan, A.P.T. Nguyen, R.V. Kayea III, S. Ziaee, G.R. Palmese, J.J. LaScala, Carbohydr. Polym. 100 (2014) 97–106.
[17] J. Li, A. Spina, J.A. Moulijn, M. Makkee, Catal. Sci. Technol. 3 (2013) 1540–1546.
[18] A. Yamaguchi, N. Hiyoshi, O. Sato, M. Shirai, Green Chem. 13 (2011) 873–881.
[19] R.M. Almeida, J. Li, C. Nederlof, P. Connor, M. Makkee, J.A. Moulijn, ChemSusChem 3 (2010) 325–328.
[20] M. Fleche, G. Huchette, Starch 38 (1986) 26–30.
[21] M. Huang, J. Luo, Z. Fang, H. Li, Appl. Catal. B 190 (2016) 103–114.
[22] X. Zhang, D. Yu, J. Zhao, W. Zhang, Y. Dong, H. Huang, Catal. Commun. 43 (2014) 29–33.
[23] I. Ahmed, N.A. Khan, D.K. Mishra, J.S. Lee, J.S. Hwang, S.H. Jhung, Chem. Eng. Sci. 93 (2013) 91–95.
[24] J. Xia, D. Yu, Y. Hu, B. Zou, P. Sun, H. Li, H. Huang, Catal. Commun. 12 (2011) 544–547.
[25] P. Sun, D.H. Yu, Y. Hu, Z.C. Tang, J.J. Xia, H. Li, H. Huang, J. Chem. Eng. 28 (2011) 99–105.
[26] R. Otomo, T. Yokoi, T. Tatsumi, Appl. Catal. A 505 (2015) 28–35.
[27] A.J. Sanborn, (Archer–Daniels–Midland Company), WO103586A, 2007.
[28] J. Zhang, L. Wang, F. Liu, X. Meng, J. Mao, F. Xiao, Catal. Today 242 (2015) 249–254.
[29] N.A. Khan, D.K. Mishra, S.S. Hwang, Y.W. Kwak, S.H. Jhung, Res. Chem. Intermed. 37 (2011) 1231–1238.
[30] J. Xi, Y. Zhang, D. Ding, Q. Xia, J. Wang, X. Liu, G. Lu, Y. Wang, Appl. Catal. A 469 (2014) 108–115.
[31] O.A. Rusu, W.F. Hoelderich, H. Wyart, M. Ibert, Appl. Catal. B 176 (2015) 139–149.
[32] M. Kurszewska, E. Skorupowa, J. Madaj, A. Konitz, A. Wojnowski, W. Wisniewski, Carbohydr. Res. 337 (2002) 1261–1268.
[33] A.A. Dabbawala, D.K. Mishra, J.S. Hwang, Catal. Commun. 42 (2013) 1–5.
[34] N. Iqbal, M. Mobin, M.Z.A. Rafiquee, J. Chem. Eng. 169 (2011) 43–49.
[35] D.P. Das, K.M. Parida, Appl. Catal. A 305 (2006) 32–38.
[36] A. Jain, A.M. Shore, S.C. Jonnalagadda, K.V. Ramanujachary, A. Mugweru, Appl. Catal. A 489 (2015) 72–76.

[37] L. Cheng, X. Guo, C. Song, G. Yu, Y. Cui, N. Xue, L. Peng, X. Guo, W. Ding, RSC Adv. 3 (2013) 23228–23235.
[38] H. Xu, Z. Miao, H. Zhao, J. Yang, J. Zhao, H. Song, N. Liang, L. Chou, Fuel 145 (2015) 234–240.
[39] G. Gliozzi, A. Innorta, A. Mancini, R. Bortolo, C. Perego, M. Ricci, F. Cavani, Appl. Catal. B 145 (2014) 24–33.
[40] O.L. Rusu, W.F. Hoelderich, H. Wyart, M. Ibert, Appl. Catal. B 176–177 (2015) 139–149.
[41] P. Sun, X.D. Long, H. He, C.G. Xia, F.W. Li, ChemSusChem 6 (2013) 1–9.
[42] A.S. Rocha, A.M.S. Forrester, M.H.C. de la Cruz, C.T. Silva, E.R. Lachter, Catal. Commun. 9 (2008) 1959–1965.
[43] R. Weingarten, G.A. Tompsett, W.C. Conner, G.W. Huber, J. Catal. 279 (2011) 174–182.
[44] A. Sinhamahapatra, N. Sutradhar, S. Pahari, H.C. Bajaj, A.B. Panda, Appl. Catal. A 394 (2011) 93–100.
[45] A.R. Hajipour, H. Karimi, Chin. J. Catal. 35 (2014) 1136–1147.
[46] E.R. Castellon, A.J. Lopez, P.M. Torres, D.I. Jones, J. Roziere, M. Trombetta, J. Solid State Chem. 175 (2003) 159–169.
[47] H.N. Kim, S.W. Keller, T.E. Mallouk, J. Schmitt, G. Decher, Chem. Mater. 9 (1997) 1414–1421.
[48] C.G. Barraclough, D.C. Bradley, J. Lewis, I.M. Thomas, J. Chem. Soc. 0 (1961) 2601–2605.
[49] H. Mao, X. Lu, M. Li, J. Yang, B. Li, Appl. Surf. Sci. 276 (2013) 787–795.
[50] R.O. Perez, R.L. Ramos, P.A. Davila, J.R. Utrilla, J. Chem. Eng. 165 (2010) 133–141.
[51] G.S. Rao, N.P. Rajan, M.H. Sekhar, S. Ammaji, K.V.R. Chary, J. Mol. Catal. A 395 (2014) 486–493.
[52] C.A. Emeis, J. Catal. 141 (1993) 347–354.
[53] A.A. Dabbawala, D.K. Mishra, G.W. Huber, J.S. Hwang, Appl. Catal. A 492 (2015) 252–261.
[54] K. Faungnawakij, R. Kikuchi, T. Matsui, T. Fukunaga, K. Eguchi, Appl. Catal. A 333 (2007) 114–121.
[55] D. Liu, P. Yuan, H. Liu, J. Cai, D. Tan, H. He, J. Zhu, T. Chen, Appl. Clay Sci. 80–81 (2013) 407–412.
[56] N.A. Khan, D.K. Mishra, I. Ahmeda, J.W. Yoon, J.S. Hwang, S.H. Jhung, Appl. Catal. A 452 (2013) 34–38.
[57] J.A. Melero, G. Morales, J. Iglesias, M. Paniagua, B. Hernández, S. Penedo, Appl. Catal. A 466 (2013) 116–122.